

# Van der Waals interaction between a microparticle and a single-wall carbon nanotube

E. V. Blagov,<sup>1</sup> G. L. Klimchitskaya,<sup>2</sup> and V. M. Mostepanenko,<sup>1</sup>

<sup>1</sup>*Noncommercial Partnership “Scientific Instruments”,*

*Tverskaya St. 11, Moscow, 103905, Russia*

<sup>2</sup>*North-West Technical University, Millionnaya St. 5, St.Petersburg, 191065, Russia*

## Abstract

The Lifshitz-type formulas describing the free energy and the force of the van der Waals interaction between an atom (molecule) and a single-wall carbon nanotube are obtained. The single-wall nanotube is considered as a cylindrical sheet carrying a two-dimensional free electron gas with appropriate boundary conditions on the electromagnetic field. The obtained formulas are used to calculate the van der Waals free energy and force between a hydrogen atom (molecule) and single-wall carbon nanotubes of different radii. Comparison studies of the van der Waals interaction of hydrogen atoms with single- and multi-wall carbon nanotubes show that depending on atom-nanotube separation distance the idealization of graphite dielectric permittivity is already applicable to nanotubes with only two or three walls.

PACS numbers: 73.22.-f, 34.50.Dy, 12.20.Ds

## I. INTRODUCTION

Van der Waals forces play a dominant role in the interaction of atoms and molecules with carbon nanostructures at separations larger than about one nanometer. These forces are of fluctuation nature and are described in second order perturbation theory as a dipole-dipole interaction. Theoretical description of the van der Waals forces as a quantum phenomenon was pioneered by London. The general theory of the van der Waals forces in the framework of quantum statistical physics was developed by Lifshitz [1, 2] using the concept of a frequency-dependent dielectric permittivity. Lifshitz's theory describes both the interaction between two semispaces or plates of finite thickness separated by a gap and between a microparticle (an atom or a molecule) and a flat surface of a macrobody. In the latter case it is commonly referred to as the Casimir-Polder force [3].

An understanding of the underlying mechanisms of microparticle—nanostructure interaction is of importance for many applications including the problem of hydrogen storage in carbon nanostructures [4]. However, the application of the Lifshitz theory to the latter case encounters serious problems because the boundary surface of carbon nanotubes is not flat and single-wall nanotubes are not characterized by the macroscopic concept of a frequency-dependent dielectric permittivity. Because of this, most theoretical work on the van der Waals interaction in layered structures and between hydrogen atoms (molecules) and a graphite sheet or carbon nanotubes was done using the phenomenological density functional theory (see, e.g., Refs. [5, 6, 7, 8, 9, 10, 11]). Some other approximate approaches were also used, e.g., the nonrelativistic perturbation theory for degenerate levels of a two-level atomic system [12, 13]. It is known, however, that in some cases the approximate and phenomenological approaches do not provide a precise description of the van der Waals interaction [14, 15]. This is true [16], for instance, when one uses the density functional theory (especially with linear-density approximation).

Recently, the scope of the Lifshitz theory of the van der Waals forces was much widened by successful application to the interpretation of precision measurements of the Casimir force [17, 18, 19, 20, 21, 22, 23] (i.e., the van der Waals force at larger separations where the relativistic retardation becomes essential) and to atom-wall interaction in connection with Bose-Einstein condensation [24, 25]. What is more, in Refs. [26, 27] the Lifshitz theory was extended for the case of an atom (molecule) interacting with a plane surface of a

uniaxial crystal or with a multi-wall carbon nanotube. The generalization to nanotubes was achieved by using the proximity force theorem [28] and the idealization of graphite dielectric permittivities which is applicable to multi-wall nanotubes with sufficiently large number of walls. In Ref. [29] the Lifshitz-type formulas were obtained for the van der Waals interaction between a single layer of graphite (hereafter, graphene) and a material plate, graphene and an atom or a molecule, and between a single-wall carbon nanotube and a plate. To achieve this goal, graphene was considered in terms of a two-dimensional free electron gas [30]. The reflection properties of electromagnetic oscillations on graphene were described by the specific boundary conditions imposed on the infinitely thin positively charged plasma sheet, carrying a continuous fluid with some mass and negative charge density [31].

In the present paper we use the same model of graphene as in Ref. [29] and obtain Lifshitz-type formulas for the van der Waals interaction between a microparticle (an atom or a molecule) and a single-wall carbon nanotube. Both the free energy and interaction force at arbitrary temperature are considered. As an example, we have calculated the van der Waals free energy and force as functions of separation in the configuration of a hydrogen atom and a molecule in close proximity to a single-wall carbon nanotube. Specifically, the values of the van der Waals coefficient are determined at different separations. Comparison studies of the van der Waals interaction of a microparticle with multi- and single-wall carbon nanotubes are performed. If we consider the van der Waals interaction of an atom or a molecule with a nanotube having only two or three walls, the idealization of the dielectric permittivity of graphite is demonstrated to be already applicable if separation distance between a microparticle and a nanotube is sufficiently large.

The paper is organized as follows. In Sec. II we derive the Lifshitz-type formulas for the van der Waals free energy and force acting between a microparticle and a single-wall carbon nanotube. Sec. III is devoted to the numerical computations of the van der Waals interaction between a hydrogen atom or a molecule and a single-wall nanotube. In Sec. IV the comparison between the cases of single- and multi-wall nanotubes is performed. Sec. V contains our conclusions and discussion.

## II. LIFSHITZ-TYPE FORMULAS FOR THE INTERACTION BETWEEN MICROPARTICLE AND SINGLE-WALL CARBON NANOTUBE

We begin with the van der Waals interaction of a graphene occupying the  $xy$ -plane,  $z = 0$ , or of a graphite plate of thickness  $d$ , with a semispace made of isotropic material. The separation distance between the graphene or the boundary plane of a graphite plate (labeled by the upper index 1) and the boundary plane of a semispace (labeled by 2) is  $a$ . As was shown in Refs. [26, 27, 29], in both cases the free energy of the van der Waals interaction per unit area at temperature  $T$  in thermal equilibrium is given by the Lifshitz-type formula with the properly defined reflection coefficients  $r_{\text{TM,TE}}^{(1,2)}$ :

$$\begin{aligned} \mathcal{F}(a, T) &= \frac{k_B T}{2\pi} \sum_{l=0}^{\infty} \left(1 - \frac{1}{2}\delta_{l0}\right) \int_0^{\infty} k_{\perp} dk_{\perp} \\ &\times \left\{ \ln \left[ 1 - r_{\text{TM}}^{(1)}(\xi_l, k_{\perp}) r_{\text{TM}}^{(2)}(\xi_l, k_{\perp}) e^{-2aq_l} \right] \right. \\ &\quad \left. + \ln \left[ 1 - r_{\text{TE}}^{(1)}(\xi_l, k_{\perp}) r_{\text{TE}}^{(2)}(\xi_l, k_{\perp}) e^{-2aq_l} \right] \right\}. \end{aligned} \quad (1)$$

Here,  $k_B$  is the Boltzmann constant,  $\xi_l = 2\pi k_B T l / \hbar$  with  $l = 1, 2, 3, \dots$  are the Matsubara frequencies along the imaginary frequency axis ( $\omega = i\xi$ ),  $k_{\perp}$  is the magnitude of the wave vector component perpendicular to the  $z$ -axis, transverse electric (TE) and transverse magnetic (TM) modes are the two independent polarizations of electromagnetic field, and  $q_l = (k_{\perp}^2 + \xi_l^2/c^2)^{1/2}$ .

From Eq. (1), the van der Waals force acting between a graphene or a graphite plate of thickness  $d$  and a semispace made of isotropic material is:

$$\begin{aligned} F(a, T) &= -\frac{\partial \mathcal{F}(a, T)}{\partial a} = -\frac{k_B T}{\pi} \sum_{l=0}^{\infty} \left(1 - \frac{1}{2}\delta_{l0}\right) \int_0^{\infty} k_{\perp} dk_{\perp} q_l \\ &\times \left[ \frac{r_{\text{TM}}^{(1)}(\xi_l, k_{\perp}) r_{\text{TM}}^{(2)}(\xi_l, k_{\perp})}{e^{2aq_l} - r_{\text{TM}}^{(1)}(\xi_l, k_{\perp}) r_{\text{TM}}^{(2)}(\xi_l, k_{\perp})} \right. \\ &\quad \left. + \frac{r_{\text{TE}}^{(1)}(\xi_l, k_{\perp}) r_{\text{TE}}^{(2)}(\xi_l, k_{\perp})}{e^{2aq_l} - r_{\text{TE}}^{(1)}(\xi_l, k_{\perp}) r_{\text{TE}}^{(2)}(\xi_l, k_{\perp})} \right]. \end{aligned} \quad (2)$$

Now we specify the reflection coefficients. For a semispace made of isotropic material (labeled by the upper index 2) they are commonly known [2, 18]

$$r_{\text{TM}}^{(2)}(\xi_l, k_{\perp}) = \frac{\varepsilon(i\xi_l)q_l - k_l}{\varepsilon(i\xi_l)q_l + k_l}, \quad r_{\text{TE}}^{(2)}(\xi_l, k_{\perp}) = \frac{k_l - q_l}{k_l + q_l}, \quad (3)$$

where

$$k_l = \sqrt{k_\perp^2 + \varepsilon(i\xi_l) \frac{\xi_l^2}{c^2}}, \quad (4)$$

and  $\varepsilon(\omega)$  is the dielectric permittivity of a semispace material.

If the first body is a graphite plate of thickness  $d$ , the reflection coefficients were found in Ref. [26]:

$$\begin{aligned} r_{\text{TM}}^{(1)}(\xi_l, k_\perp) &= r_{\text{TM},d}^{(1)}(\xi_l, k_\perp) = \frac{\varepsilon_x(i\xi_l)\varepsilon_z(i\xi_l)q_l^2 - k_{z_l}^2}{\varepsilon_x(i\xi_l)\varepsilon_z(i\xi_l)q_l^2 + k_{z_l}^2 + 2q_l k_{z_l} \sqrt{\varepsilon_x(i\xi_l)\varepsilon_z(i\xi_l)} \coth(k_{z_l}d)}, \\ r_{\text{TE}}^{(1)}(\xi_l, k_\perp) &= r_{\text{TE},d}^{(1)}(\xi_l, k_\perp) = \frac{k_{x_l}^2 - q_l^2}{k_{x_l}^2 + q_l^2 + 2q_l k_{x_l} \coth(k_{x_l}d)}. \end{aligned} \quad (5)$$

Here,  $\varepsilon_x(\omega) = \varepsilon_y(\omega)$  and  $\varepsilon_z(\omega)$  are the dielectric permittivities of graphite in the  $x$ ,  $y$  and  $z$  directions, respectively, and

$$k_{x_l} = \sqrt{k_\perp^2 + \varepsilon_x(i\xi_l) \frac{\xi_l^2}{c^2}}, \quad k_{z_l} = \sqrt{k_\perp^2 + \varepsilon_z(i\xi_l) \frac{\xi_l^2}{c^2}}. \quad (6)$$

If the first body is graphene, the idealization of the frequency-dependent dielectric permittivity cannot be used. In this case the reflection coefficients can be found [29, 31, 32] by modeling graphene as a two-dimensional plasma sheet carrying a negatively charged fluid of  $\pi$ -electrons. For the hexagonal structure of carbon layers there is one  $\pi$ -electron per atom [33] resulting in two  $\pi$ -electrons per one hexagonal cell. This leads to the following values for the density of  $\pi$ -electrons and the wave number of the sheet:

$$n = \frac{4}{3\sqrt{3}l^2}, \quad K = 2\pi \frac{ne^2}{mc^2} = 6.75 \times 10^5 \text{ m}^{-1}, \quad (7)$$

where  $l = 1.421 \text{ \AA}$  is the side length of a hexagon,  $e$  and  $m$  are the electron charge and mass, respectively.

Now we are solving the Maxwell equations with the following matching conditions on the tangential and normal components of the fields:

$$\begin{aligned} \mathbf{E}_{t,2} - \mathbf{E}_{t,1} &= 0, \quad E_{z,2} - E_{z,1} = 2K \frac{c^2}{\omega^2} \nabla_t \cdot \mathbf{E}_t, \\ B_{z,2} - B_{z,1} &= 0, \quad \mathbf{B}_{t,2} - \mathbf{B}_{t,1} = -2iK \frac{c}{\omega} \mathbf{j} \times \mathbf{E}_t. \end{aligned} \quad (8)$$

Here  $\mathbf{j} = (0, 0, 1)$  is the unit vector pointing in  $z$ -direction, and all fields depend on time through a common factor  $\exp(-i\omega t)$ . As a result, we arrive to one-dimensional scattering

problem in the  $z$ -direction [18]. The solution of this problem leads to the following reflection coefficients on a graphene sheet [29, 31, 32]:

$$\begin{aligned} r_{\text{TM}}^{(1)}(\xi_l, k_\perp) &= r_{\text{TM},g}^{(1)}(\xi_l, k_\perp) = \frac{c^2 q_l K}{c^2 q_l K + \xi_l^2}, \\ r_{\text{TE}}^{(1)}(\xi_l, k_\perp) &= r_{\text{TE},g}^{(1)}(\xi_l, k_\perp) = \frac{K}{K + q_l}. \end{aligned} \quad (9)$$

Now we use Eqs. (1) and (2) with the reflection coefficients (3) and (9) to obtain the free energy of van der Waals interaction and force acting between an atom (molecule) and a single-wall carbon nanotube. For this purpose let us consider an infinite space filled with an isotropic substance having a dielectric permittivity  $\varepsilon(\omega)$  containing an empty cylindrical cavity of radius  $R + a$ . We introduce the single-wall carbon nanotube of radius  $R$  inside this cavity (see Fig. 1). In so doing the nanotube is modeled by a cylindrical graphene sheet. Then there is a gap of thickness  $a$  between the nanotube and the boundary surface of the cylindrical cavity. Each element of the nanotube experiences an attractive van der Waals force on the source side of this boundary surface. By using the proximity force approximation (see Ref. [34] in the case of ideal metals), the free energy of the van der Waals interaction between these two co-axial cylinders can be approximately represented in the form

$$\mathcal{F}^{c,c}(a, T) = 2\pi L \sqrt{R(R + a)} \mathcal{F}(a, T). \quad (10)$$

Here  $\mathcal{F}(a, T)$  is the free energy per unit area in the configuration of a graphene interacting with a plane boundary of an isotropic semispace determined in Eq. (1), and  $L$  is the length of the nanotube, which is supposed to be much larger than  $R$ .

The accuracy of Eq. (10) is rather high. Recently the accuracy of the proximity force approximation was investigated on the basis of first principles by comparing the approximate results with the exact ones for the configurations of a cylinder or a sphere above plate. It was shown [35, 36, 37, 38] that corrections to the results obtained using the proximity force approximation are less than  $0.5a/R$  where  $R$  is a cylinder or sphere radius. For the configuration of two co-axial cylinders the accuracy of the proximity force approximation is even much higher. For example, within the separation region  $0 < a < R/2$ , the results calculated using Eq. (10) coincide with the exact ones up to 1% for cylinders made of ideal metal [34, 39] (for real materials the accuracy may be different for only a fraction of a percent).

To come to the case of an atom (or molecule) near a nanotube, we suppose that the isotropic substance filling the infinite space is rarefied with some small number  $N$  of atoms (molecules) per unit volume. We expand the quantity  $\mathcal{F}^{c,c}(a, T)$  on the left-hand side of Eq. (10) in powers of  $N$  and using the additivity of the first-order term arrive at:

$$\mathcal{F}^{c,c}(a, T) = N \int_a^\infty \mathcal{F}^{a,c}(z, T) 2\pi(R+z)L dz + O(N^2). \quad (11)$$

Here,  $\mathcal{F}^{a,c}(z, T)$  is (yet not found) the free energy of the van der Waals interaction of a single atom (molecule) belonging to an isotropic substance with a single-wall carbon nanotube ( $z$  is measured from the external surface of nanotube in the direction perpendicular to it).

Differentiation of both (negative) sides of Eq. (11) with respect to  $a$  leads to:

$$-\frac{\partial \mathcal{F}^{c,c}(a, T)}{\partial a} = 2\pi(R+a)LN \mathcal{F}^{a,c}(a, T) + O(N^2). \quad (12)$$

This negative derivative can be found also by the differentiation of both sides of Eq. (10):

$$\begin{aligned} -\frac{\partial \mathcal{F}^{c,c}(a, T)}{\partial a} &= 2\pi L \sqrt{R(R+a)} \\ &\times \left[ -\frac{1}{2(R+a)} \mathcal{F}(a, T) + F(a, T) \right], \end{aligned} \quad (13)$$

where the force  $F(a, T)$  acting between a graphene and a semispace was defined in Eq. (2) with the reflection coefficients (3) and (9).

We expand the dielectric permittivity of a rarefied substance in powers of  $N$  [40]

$$\varepsilon(i\xi_l) = 1 + 4\pi\alpha(i\xi_l)N + O(N^2), \quad (14)$$

where  $\alpha(\omega)$  is the dynamic polarizability of an atom or a molecule of this substance. Using Eq. (14), we expand also the reflection coefficients  $r_{\text{TM,TE}}^{(2)}(\xi_l, k_\perp)$  in Eq. (3) in powers of  $N$  and substitute the obtained expressions in Eqs. (1) and (2). Thereafter, with the help of Eqs. (13) and (12) in the limit  $N \rightarrow 0$ , the desired expression for the van der Waals free energy in the configuration of a microparticle interacting with a single-wall carbon nanotube is obtained (see Ref. [26] devoted to multi-wall nanotubes for the details of perturbation expansion and limiting procedure):

$$\begin{aligned} \mathcal{F}^{a,c}(a, T) &= -k_B T \sqrt{\frac{R}{R+a}} \sum_{l=0}^{\infty} \left( 1 - \frac{1}{2} \delta_{l0} \right) \alpha(i\xi_l) \\ &\times \int_0^\infty k_\perp dk_\perp e^{-2aq_l} \left[ q_l - \frac{1}{4(R+a)} \right] \\ &\times \left\{ 2r_{\text{TM},g}^{(1)}(\xi_l, k_\perp) + \frac{\xi_l^2}{q_l^2 c^2} \left[ r_{\text{TE},g}^{(1)}(\xi_l, k_\perp) - r_{\text{TM},g}^{(1)}(\xi_l, k_\perp) \right] \right\}. \end{aligned} \quad (15)$$

In the limiting case  $R \rightarrow \infty$ , Eq. (15) coincides with a known result for the free energy of a microparticle near a plane surface of graphene [29]. If, instead of graphene, the cylindrical graphite shell of thickness  $d$  is considered, Eq. (15) describes [26] the interaction of a microparticle with such a shell if the reflection coefficients  $r_{\text{TM,TE},g}^{(1)}(\xi_l, k_\perp)$  are replaced with  $r_{\text{TM,TE},d}^{(1)}(\xi_l, k_\perp)$  defined in Eq. (5).

The van der Waals force acting between a microparticle and a single-wall carbon nanotube is obtained as a minus derivative of Eq. (15) with respect to separation distance

$$\begin{aligned}
F^{a,c}(a, T) &= -k_B T \sqrt{\frac{R}{R+a}} \sum_{l=0}^{\infty} \left(1 - \frac{1}{2} \delta_{l0}\right) \alpha(i\xi_l) \\
&\times \int_0^{\infty} k_\perp dk_\perp e^{-2aq_l} \left[2q_l^2 - \frac{3}{8(R+a)^2}\right] \\
&\times \left\{2r_{\text{TM},g}^{(1)}(\xi_l, k_\perp) + \frac{\xi_l^2}{q_l^2 c^2} \left[r_{\text{TE},g}^{(1)}(\xi_l, k_\perp) - r_{\text{TM},g}^{(1)}(\xi_l, k_\perp)\right]\right\}.
\end{aligned} \tag{16}$$

By replacing the reflection coefficients  $r_{\text{TM,TE},g}^{(1)}(\xi_l, k_\perp)$  with  $r_{\text{TM,TE},d}^{(1)}(\xi_l, k_\perp)$  we return to the expression for the force between a microparticle and a graphite cylindrical shell of thickness  $d$  [26].

### III. CALCULATION OF THE VAN DER WAALS INTERACTION BETWEEN HYDROGEN ATOM OR MOLECULE AND SINGLE-WALL CARBON NANOTUBE

For the purpose of numerical computations it is convenient to introduce the nondimensional variables under the integrals

$$y = 2aq_l, \quad \zeta_l = \frac{2a\xi_l}{c} \equiv \frac{\xi_l}{\omega_c} \tag{17}$$

and present the free energy (15) and force (16) in the form

$$\mathcal{F}^{a,c}(a, T) = -\frac{C_3(a, T)}{a^3}, \quad F^{a,c}(a, T) = -\frac{C_F(a, T)}{a^4}, \tag{18}$$

where

$$\begin{aligned}
C_3(a, T) = & \frac{k_B T}{8} \sqrt{\frac{R}{R+a}} \left\{ \frac{4R+3a}{2(R+a)} \alpha(0) \right. \\
& + \sum_{l=1}^{\infty} \alpha(i\xi_l) \int_{\zeta_l}^{\infty} dy y e^{-y} \left[ y - \frac{a}{2(R+a)} \right] \\
& \times \left[ 2r_{\text{TM},g}^{(1)}(\zeta_l, y) + \frac{\zeta_l^2}{y^2} \left( r_{\text{TE},g}^{(1)}(\zeta_l, y) - r_{\text{TM},g}^{(1)}(\zeta_l, y) \right) \right] \left. \right\}, \tag{19}
\end{aligned}$$

$$\begin{aligned}
C_F(a, T) = & \frac{k_B T}{8} \sqrt{\frac{R}{R+a}} \left\{ \frac{3(2R+3a)(2R+a)}{2(R+a)^2} \alpha(0) \right. \\
& + \sum_{l=1}^{\infty} \alpha(i\xi_l) \int_{\zeta_l}^{\infty} dy y e^{-y} \left[ y^2 - \frac{3a^2}{4(R+a)^2} \right] \\
& \times \left[ 2r_{\text{TM},g}^{(1)}(\zeta_l, y) + \frac{\zeta_l^2}{y^2} \left( r_{\text{TE},g}^{(1)}(\zeta_l, y) - r_{\text{TM},g}^{(1)}(\zeta_l, y) \right) \right] \left. \right\}. \tag{20}
\end{aligned}$$

In terms of new variables (17) the reflection coefficients (9) take the form

$$\begin{aligned}
r_{\text{TM},g}^{(1)}(\zeta_l, y) &= \frac{2yaK}{2yaK + \zeta_l^2}, \tag{21} \\
r_{\text{TE},g}^{(1)}(\zeta_l, y) &\equiv r_{\text{TE},g}^{(1)}(y) = \frac{2aK}{2aK + y}.
\end{aligned}$$

To perform computations using Eqs. (19) and (20) one needs some expressions for the atomic and molecular dynamic polarizabilities of hydrogen. As was shown in Refs. [26, 41], for the calculation of van der Waals interaction the polarizabilities can be represented with sufficient precision in the framework of the single-oscillator model,

$$\begin{aligned}
\alpha(i\xi_l) = \alpha_a(i\xi_l) &= \frac{g_a}{\omega_a^2 + \xi_l^2}, \tag{22} \\
\alpha(i\xi_l) = \alpha_m(i\xi_l) &= \frac{g_m}{\omega_m^2 + \xi_l^2},
\end{aligned}$$

for a hydrogen atom and a molecule, respectively. Here,  $g_a = \alpha_a(0)\omega_a^2$  with the static atomic polarizability of hydrogen equal to  $\alpha_a(0) = 4.50$  a.u. and the characteristic frequency  $\omega_a = 11.65$  eV [42]. For a hydrogen molecule it holds  $g_m = \alpha_m(0)\omega_m^2$  with  $\alpha_m(0) = 5.439$  a.u. and  $\omega_m = 14.09$  eV [42]. Note that when substituting polarizabilities in Eqs. (19), (20), they should be expressed in cubic meters (1 a.u. of polarizability is equal to  $1.482 \times 10^{-31}$  m<sup>3</sup>).

The computations were performed for single-wall carbon nanotubes with radii  $R = 2, 3, 4$  and 5 nm at  $T = 300$  K. As an example, in Fig. 2 we plot the van der Waals coefficient (19) as a function of separation in the region from 1 to 3 nm for the nanotube with  $R = 5$  nm. Solid line 1 labels a nanotube interaction with a hydrogen atom and solid line 2 with a hydrogen

molecule. For comparison, in the same figure the previously computed [29] van der Waals coefficients for the interaction of a hydrogen atom (the dashed line 1) and molecule (the dashed line 2) with a plane graphene sheet are included. As is seen in Fig. 2 (the solid lines 1 and 2), at all separations the van der Waals coefficient of a molecule-nanotube interaction is larger than of an atom-nanotube interaction. At the same time, the van der Waals coefficients for the interaction of a hydrogen atom or a molecule with graphene (the dashed lines 1 and 2, respectively) are larger than the respective coefficients for the interaction with a single-wall carbon nanotube. This excess is of about 30%. Note that the obtained results practically do not depend on temperature in the temperature region from 0 to 300 K.

In Table I we present a few computational results for the van der Waals coefficient  $C_3$  in the case of hydrogen atom (columns 2–5) and molecule (columns 6–9) interacting with single-wall carbon nanotubes of different radii. From Table I it is seen that the van der Waals coefficient  $C_3$  is monotonously increasing with the increase of nanotube radius. As in Fig. 2, the separation distance between an atom (molecule) and a nanotube varies from 1 to 3 nm (recall that at shorter separations some additional forces of chemical and exchange nature should be taken into account; at larger separations the accuracy of the obtained theoretical expressions may decrease).

In Fig. 3 we plot the coefficient  $C_F$  for the van der Waals force defined in Eq. (20) acting between a hydrogen atom (the solid line 1) or a molecule (the solid line 2) interacting with the single-wall carbon nanotube of  $R = 5$  nm radius. As it holds for the coefficient  $C_3$ , the values of the coefficient  $C_F$  for a molecule are larger than for an atom at all separations under consideration. Dotted lines in Fig. 3 (labeled 1 for an atom and 2 for a molecule) represent the results obtained on the assumption that  $C_F = 3C_3$ , i.e., on the assumption that the van der Waals coefficient  $C_3 = \text{const}$  and does not depend on separation distance. As is seen in Fig. 3, the differences between solid and dotted lines are of about 15–20%. Thus, the dependence of the van der Waals coefficients on separation in atom (molecule)—nanotube interaction is essential for obtaining the computational results of high precision.

In Table II the computational results for the van der Waals force coefficient  $C_F$  are presented. Columns 2–5 are related to the case of hydrogen atom and columns 6–9 to hydrogen molecule interacting with single-wall carbon nanotubes of radii  $R = 2, 3, 4$  and 5 nm. As in Table I, the separation distance varies from 1 to 3 nm. From Table II it is seen that the magnitudes of the coefficient  $C_F$  increase with the increase of a nanotube radius

and decrease with the increase of separation distance. The respective magnitudes of  $C_F$  for a hydrogen molecule are larger than for an atom for nanotubes of different radii.

#### IV. COMPARISON OF INTERACTIONS BETWEEN HYDROGEN ATOM (MOLECULE) AND CARBON NANOTUBE IN THE CASES OF SINGLE- AND MULTI-WALL NANOTUBES

In this section we compare the van der Waals coefficients for the interaction of hydrogen atom or molecule with single-wall and multi-wall carbon nanotubes. This permits us to determine how thick should be a multi-wall nanotube in order the idealization of the dielectric permittivities of graphite be applicable. We will also quantitatively compare the cases of multi-wall and single-wall carbon nanotubes depending on the separation distance between a nanotube and a microparticle.

The van der Waals coefficient of the interaction between a single-wall nanotube and a microparticle is given by Eq. (19) with reflection coefficients (21). To obtain the van der Waals coefficient of the interaction with a multi-wall nanotube, one should replace the reflection coefficients  $r_{\text{TM,TE},g}^{(1)}$  in Eq. (19) with the coefficients  $r_{\text{TM,TE},d}^{(1)}$  defined in Eq. (5) [26]. In terms of dimensionless variables (17) the latter take the form

$$\begin{aligned} r_{\text{TM},d}^{(1)}(\zeta_l, y) &= \frac{\varepsilon_{xl}\varepsilon_{zl}y^2 - f_z^2(y, \zeta_l)}{\varepsilon_{xl}\varepsilon_{zl}y^2 + f_z^2(y, \zeta_l) + 2\sqrt{\varepsilon_{xl}\varepsilon_{zl}}yf_z(y, \zeta_l) \coth [f_z(y, \zeta_l)d/(2a)]}, \\ r_{\text{TE},d}^{(1)}(\zeta_l, y) &= \frac{f_x^2(y, \zeta_l) - y^2}{y^2 + f_x^2(y, \zeta_l) + 2yf_x(y, \zeta_l) \coth [f_x(y, \zeta_l)d/(2a)]}, \end{aligned} \quad (23)$$

where the following notations are introduced

$$\begin{aligned} \varepsilon_{xl} &\equiv \varepsilon_x(i\zeta_l\omega_c), & \varepsilon_{zl} &\equiv \varepsilon_z(i\zeta_l\omega_c), \\ f_z^2(y, \zeta_l) &= y^2 + \zeta_l^2(\varepsilon_{zl} - 1), & f_x^2(y, \zeta_l) &= y^2 + \zeta_l^2(\varepsilon_{xl} - 1). \end{aligned} \quad (24)$$

The computational results for the van der Waals coefficient  $C_3$  of atom-nanotube interaction are presented in Fig. 4 by the solid dots 1, 2, 3 (the single-wall carbon nanotube of 5 nm radius at separations  $a = 1, 2$  and  $3$  nm to a hydrogen atom, respectively) and by the solid dots connected with solid lines for the multi-wall carbon nanotubes of 5 nm external radius with  $n = 1, 2, 3, 4$  and  $5$  walls, respectively. For a single-wall nanotube computations were performed using Eqs. (19), (21) and for a multi-wall nanotubes using Eqs. (19), (23). In

both cases the dynamic atomic polarizability  $\alpha_a$  is taken in Eq. (22) and for a multi-wall nanotube  $d = 3.4(n-1) \text{ \AA}$ . As is seen in Fig. 4, the van der Waals coefficient computed by the formula for a multi-wall nanotube with only one wall does not coincide with the coefficient computed by the formula for a single-wall nanotube. This is expected result because the reflection coefficients in Eq. (23) approach zero when the nanotube thickness  $d$  vanishes. At the same time, as Fig. 4 suggests, the van der Waals coefficients for a multi-wall nanotube with  $n = 3$  walls at 1 nm from an atom and for a multi-wall nanotube with  $n = 2$  walls at a separation 2 or 3 nm from an atom are in the proper proportion to the coefficients computed for a single-wall nanotube using the reflection coefficients (21) (the analogical result was obtained in Ref. [29] for the interaction of a graphene and a graphite plate with an Au semispace). This permits us to conclude that the macroscopic concept of graphite dielectric permittivity used in Ref. [26] to describe multi-wall carbon nanotubes is already applicable for nanotubes containing only two or three walls depending on separation distance between a nanotube and an atom.

Fig. 5 contains the same information, as in Fig. 4, but for a hydrogen molecule. It is seen that the approximation of graphite dielectric permittivities is also well applicable for multi-wall nanotube with 3 walls spaced 1 nm apart from a molecule and for two-wall nanotube at a separation of 2 or 3 nm from a molecule. The values of the van der Waals coefficient for a molecule are, however, larger than for an atom in accordance to Sec. III. The single-wall nanotube cannot be described using the macroscopic concept of dielectric permittivity but as a cylindrical plasma sheet with appropriate boundary conditions.

## V. CONCLUSIONS AND DISCUSSION

In the foregoing, we have obtained the Lifshitz-type formulas describing the free energy and force of the van der Waals interaction of a hydrogen atom or a molecule with a single-wall carbon nanotube. The nanotube is represented using the description of a cylindrical graphene sheet in terms of two-dimensional plasma carrying free  $\pi$ -electrons with appropriate boundary conditions imposed on the electromagnetic field. Recently this approach was used to describe the interaction of a flat graphene sheet with a material plate or a microparticle, and a material plate with a single-wall carbon nanotube [29]. The formulas obtained here were applied to calculate the van der Waals free energy and force in the configuration

of a hydrogen atom or a molecule interacting with single-wall carbon nanotubes of different radii. The comparison with the previously developed Lifshitz-type formalism applicable to multi-wall carbon nanotubes [26] have allowed to determine the application limits of the macroscopic concept of graphite dielectric permittivity. The latter was shown to be applicable even to two- or three-wall nanotubes depending on the separation distance between a nanotube and an atom (molecule).

The developed formalism suggests some advantages in comparison to phenomenological and semi-phenomenological approaches used to calculate the van der Waals interaction. As was recently noted in Ref. [11], the phenomenological method of pairwise summation of the intermolecular van der Waals potentials can lead to even qualitatively wrong results for the nonretarded van der Waals interaction between metallic nanotubes and nanowires (in Ref. [43] it was emphasized that the pairwise summation of intermolecular potentials leads to correct dependence of the van der Waals potential and force on separation distance only for bulk three-dimensional bodies).

The possibility to use the Lifshitz theory of dispersion forces for the investigation of the van der Waals interaction between hydrogen atoms (molecules) and single-wall carbon nanotubes demonstrated in the paper may be helpful for the problem of hydrogen storage. According to recent review on the subject [44], there are conceptual possibilities to create carbon nanostructures capable of absorbing more than 10 mass % of hydrogen. The resolution of this fundamental problem requires a detailed investigation of the microscopic mechanisms of the interaction between hydrogen and graphite. To attain these ends the above approach should be extended to distances below 1 nm. At so small separations there may be attractive chemical forces and short-range repulsive forces of exchange nature. These forces depend on atomic structure and cannot be taken into account by means of the boundary conditions. Some approximate description is possible by combining the energy of van der Waals attraction with phenomenological potentials [45].

### **Acknowledgments**

This work was supported by the Russian Foundation for Basic Research (Grant No. 05-08-18119a). G.L.K. and V.M.M. were also partially supported by Deutsche Forschungs-

gemeinschaft (Grant No. 436 RUS 113/789/0–3).

---

- [1] E. M. Lifshitz, Zh. Eksp. Teor. Fiz. **29**, 94 (1956) [Sov. Phys. JETP **2**, 73 (1956)].
- [2] E. M. Lifshitz and L. P. Pitaevskii, *Statistical Physics* (Pergamon Press, Oxford, 1980), Pt. II.
- [3] H. B. G. Casimir and D. Polder, Phys. Rev. **73**, 360 (1948).
- [4] A. C. Dillon, K. M. Jones, T. A. Bekkedahl, C. H. Kiang, D. S. Bethune, and M. J. Heben, Nature **386**, 377 (1997).
- [5] W. A. Diño, H. Nakanishi, and H. Kasai, e-J. Surf. Sci. Nanotech. **2**, 77 (2004).
- [6] A. Bogicevic, S. Ovesson, P. Hyldgaard, B. I. Lundqvist, H. Brune, and D. R. Jennison, Phys. Rev. Lett. **85**, 1910 (2000).
- [7] E. Hult, P. Hyldgaard, and B. I. Lundqvist, Phys. Rev. B **64**, 195414 (2001).
- [8] H. Rydberg, M. Dion, N. Jacobson, E. Schröder, P. Hyldgaard, S. I. Simak, D. C. Landreth, and B. I. Lundqvist, Phys. Rev. Lett. **91**, 126402 (2003).
- [9] J. Jung, P. García-González, J. F. Dobson, and R. W. Godby, Phys. Rev. B **70**, 205107 (2004).
- [10] J. Kleis, P. Hyldgaard, and E. Schröder, Comp. Mat. Sci. **33**, 192 (2005).
- [11] J. F. Dobson, A. White, and A. Rubio, Phys. Rev. Lett. **96**, 073201 (2006).
- [12] I. V. Bondarev and Ph. Lambin, Solid State Commun. **132**, 203 (2004).
- [13] I. V. Bondarev and Ph. Lambin, Phys. Rev. B **72**, 035451 (2005).
- [14] J. Mahanty and B. W. Ninham, *Dispersion Forces* (Academic Press, New York, 1976).
- [15] V. A. Parsegian, *Van der Waals forces: A Handbook for Biologists, Chemists, Engineers, and Physicists* (Cambridge University Press, Cambridge, 2005).
- [16] L. A. Girifalco and M. Hodak, Phys. Rev. B **65**, 125404 (2002).
- [17] G. L. Klimchitskaya, A. Roy, U. Mohideen, and V. M. Mostepanenko, Phys. Rev. A **60**, 3487 (1999).
- [18] M. Bordag, U. Mohideen, and V. M. Mostepanenko, Phys. Rep. **353**, 1 (2001).
- [19] F. Chen, U. Mohideen, G. L. Klimchitskaya, and V. M. Mostepanenko, Phys. Rev. Lett. **88**, 101801 (2002); Phys. Rev. A **66**, 032113 (2002).
- [20] R. S. Decca, E. Fischbach, G. L. Klimchitskaya, D. E. Krause, D. López, and V. M. Mostepanenko, Phys. Rev. D **68**, 116003 (2003); Ann. Phys. (N.Y.) **318**, 37 (2005).

- [21] F. Chen, G. L. Klimchitskaya, U. Mohideen, and V. M. Mostepanenko, Phys. Rev. A **69**, 022117 (2004).
- [22] F. Chen, U. Mohideen, G. L. Klimchitskaya, and V. M. Mostepanenko, Phys. Rev. A **72**, 020101(R) (2005); **74**, 022103 (2006).
- [23] F. Chen, G. L. Klimchitskaya, V. M. Mostepanenko, and U. Mohideen, Phys. Rev. Lett. **97**, 170402 (2006).
- [24] J. F. Babb, G. L. Klimchitskaya, and V. M. Mostepanenko, Phys. Rev. A **70**, 042901 (2004).
- [25] M. Antezza, L. P. Pitaevskii, and S. Stringari, Phys. Rev. A **70**, 053619 (2004).
- [26] E. V. Blagov, G. L. Klimchitskaya, and V. M. Mostepanenko, Phys. Rev. B **71**, 235401 (2005).
- [27] G. L. Klimchitskaya, E. V. Blagov, and V. M. Mostepanenko, J. Phys. A: Math. Gen. **39**, 6481 (2006).
- [28] J. Blocki, J. Randrup, W. J. Swiatecki, and C. F. Tsang, Ann. Phys. (N.Y.) **105**, 427 (1977).
- [29] M. Bordag, B. Geyer, G. L. Klimchitskaya, and V. M. Mostepanenko, Phys. Rev. B **74**, 205431 (2006).
- [30] A. L. Fetter, Ann. Phys. (N.Y.) **81**, 367 (1973).
- [31] G. Barton, J. Phys. A: Math. Gen. **37**, 1011 (2004); **38**, 2997 (2005).
- [32] M. Bordag, J. Phys. A: Math. Gen. **39**, 6173 (2006).
- [33] G. A. Gallup, Chem. Phys. Lett. **187**, 187 (1991).
- [34] F. D. Mazzitelli, in: Quantum Field Theory Under the Influence of External Conditions, ed. K. A. Milton (Rinton Press, Princeton, 2004).
- [35] T. Emig, R. L. Jaffe, M. Kardar, and A. Scardicchio, Phys. Rev. Lett. **96**, 080403 (2006).
- [36] A. Bulgac, P. Magierski, and A. Wirzba, Phys. Rev. D **73**, 025007 (2006).
- [37] M. Bordag, Phys. Rev. D **73**, 125018 (2006).
- [38] H. Gies and K. Klingmüller, Phys. Rev. Lett. **96**, 220401 (2006); Phys. Rev. D **74**, 045002 (2006).
- [39] F. D. Mazzitelli, M. J. Sanchez, N. Scoccola, and J. Von Stecher, Phys. Rev. A **67**, 013807 (2003).
- [40] L. D. Landau, E. M. Lifshitz, and L. P. Pitaevskii, *Electrodynamics of Continuous Media* (Pergamon Press, Oxford, 1984).
- [41] A. O. Caride, G. L. Klimchitskaya, V. M. Mostepanenko, and S. I. Zanette, Phys. Rev. A **71**, 042901 (2005).

- [42] A. Rauber, J. R. Klein, M. W. Cole, and L. W. Bruch, *Surf. Sci.* **123**, 173 (1982).
- [43] V. M. Mostepanenko and N. N. Trunov, *The Casimir Effect and Its Applications* (Clarendon Press, Oxford, 1997).
- [44] Yu. S. Nechaev, *Physics — Uspekhi* **49**, 563 (2006).
- [45] J. Israelachvili, *Intermolecular and Surface Forces* (Academic Press, New York, 1992).

## Figures

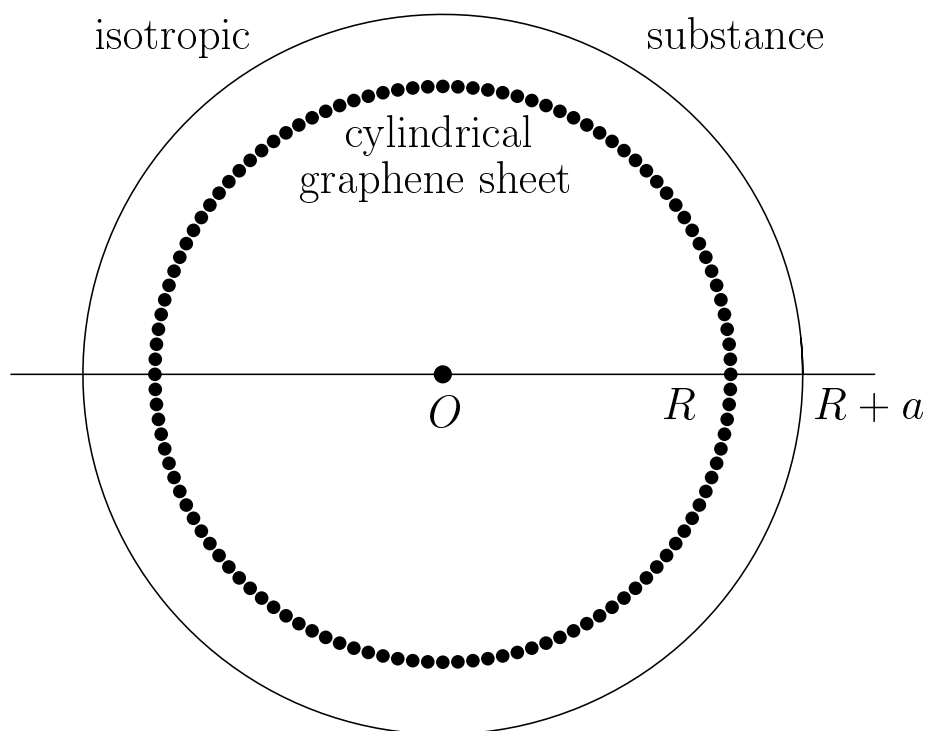


FIG. 1: Schematic of the cylindrical graphene sheet of radius  $R$  which is concentrically placed into a cylindrical cavity of radius  $R + a$  in the infinite space filled with an isotropic substance.

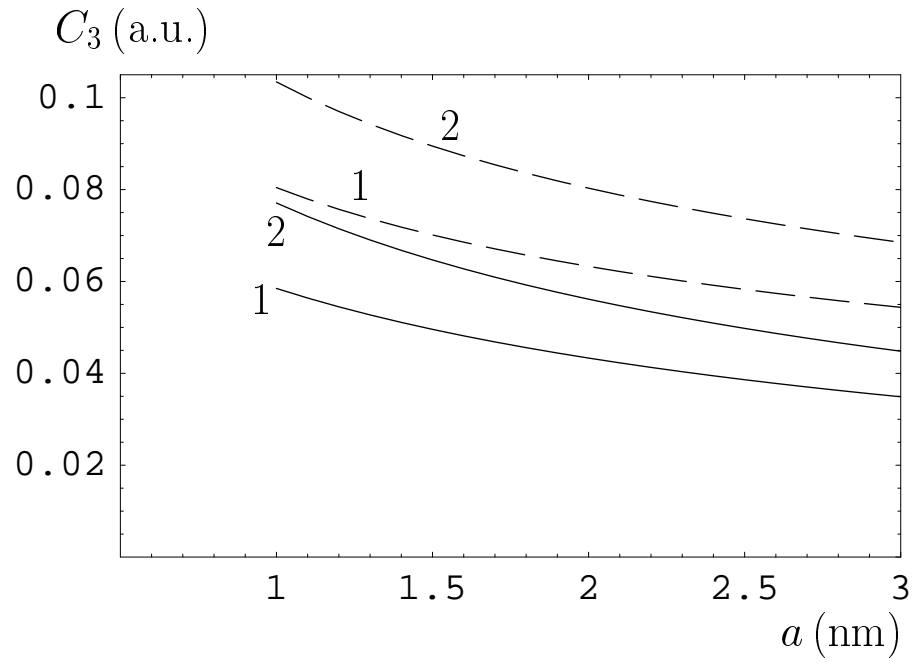


FIG. 2: The van der Waals coefficient as a function of separation for the interaction of a hydrogen atom (lines labeled 1) or a molecule (lines labeled 2) with the single-wall carbon nanotube of  $R = 5$  nm radius (solid lines) and with a plane graphene sheet (dashed lines).

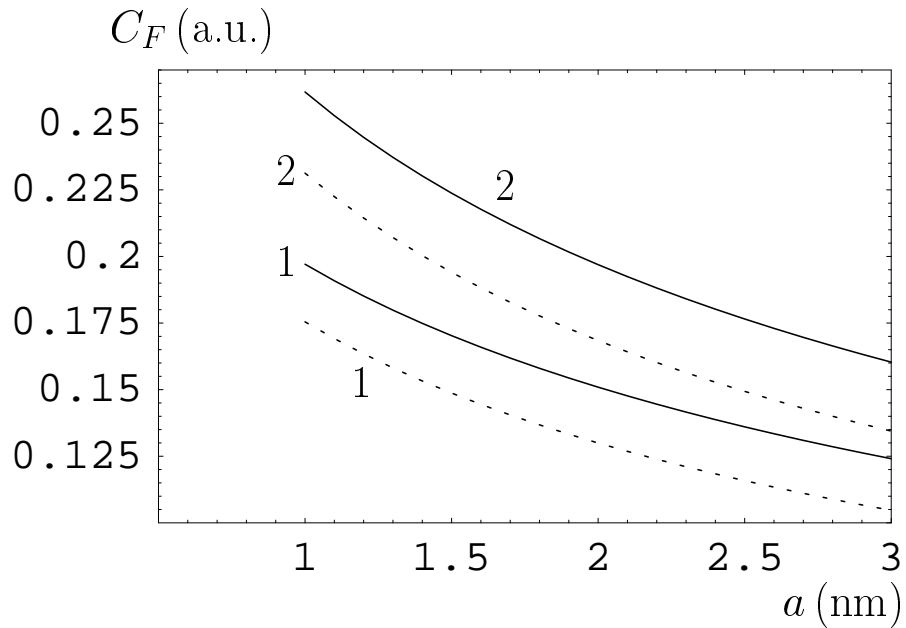


FIG. 3: The coefficient  $C_F$  as a function of separation for the interaction of a hydrogen atom (lines labeled 1) or a molecule (lines labeled 2) with the single-wall carbon nanotube of  $R = 5$  nm radius (solid lines). Dotted lines are drawn under the assumption that  $C_F = 3C_3$ , i.e., that the van der Waals coefficient  $C_3$  does not depend on separation.

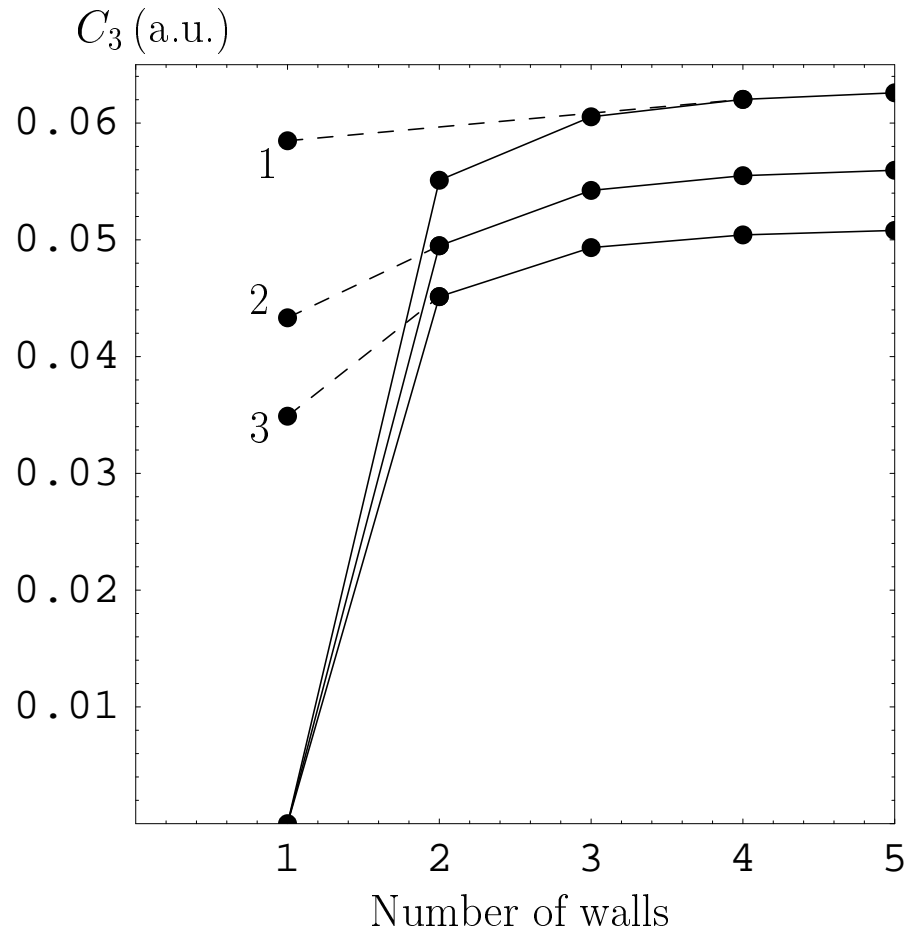


FIG. 4: The van der Waals coefficient as a function of the number of walls for the interaction of a hydrogen atom with the multi-wall carbon nanotube of  $R = 5$  nm external radius (solid dots connected with solid lines) and with a single-wall carbon nanotube of the same radius (solid dots 1, 2, 3) spaced at 1, 2 and 3 nm from the atom, respectively.

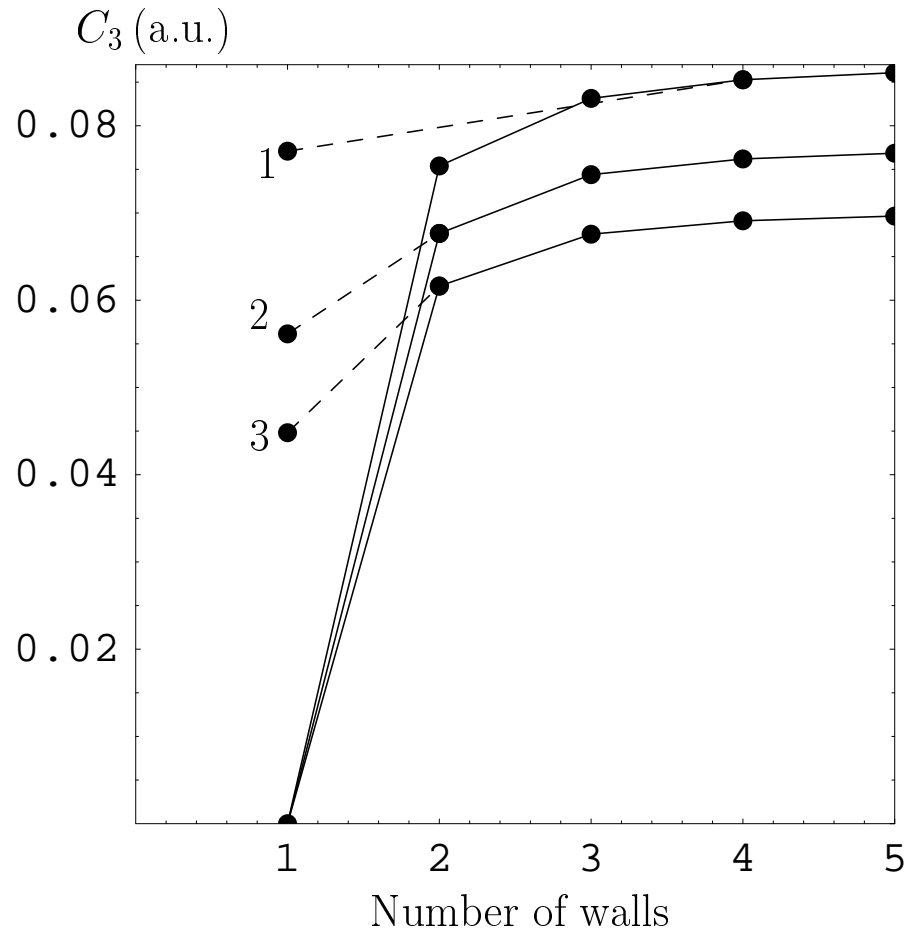


FIG. 5: The van der Waals coefficient as a function of the number of walls for the interaction of a hydrogen molecule with the multi-wall carbon nanotube of  $R = 5$  nm external radius (solid dots connected with solid lines) and with a single-wall carbon nanotube of the same radius (solid dots 1, 2, 3) spaced at 1, 2 and 3 nm from the molecule, respectively.

## Tables

TABLE I: The van der Waals coefficient as a function of separation for the interaction of a hydrogen atom or a molecule with single-wall carbon nanotubes of different radii.

$a$ (nm)	$C_3$ (a.u.)							
	hydrogen atom				hydrogen molecule			
	$R = 2$ nm	$R = 3$ nm	$R = 4$ nm	$R = 5$ nm	$R = 2$ nm	$R = 3$ nm	$R = 4$ nm	$R = 5$ nm
1.0	0.0503	0.0544	0.0569	0.0585	0.0664	0.0718	0.0750	0.0771
1.2	0.0460	0.0502	0.0528	0.0545	0.0604	0.0659	0.0692	0.0715
1.4	0.0424	0.0466	0.0493	0.0511	0.0554	0.0610	0.0644	0.0668
1.6	0.0393	0.0436	0.0463	0.0482	0.0513	0.0568	0.0603	0.0627
1.8	0.0367	0.0410	0.0437	0.0456	0.0478	0.0532	0.0568	0.0592
2.0	0.0345	0.0387	0.0414	0.0433	0.0477	0.0501	0.0536	0.0561
2.2	0.0325	0.0366	0.0394	0.0413	0.0420	0.0474	0.0509	0.0534
2.4	0.0307	0.0348	0.0375	0.0395	0.0397	0.0449	0.0484	0.0509
2.6	0.0292	0.0332	0.0358	0.0378	0.0376	0.0427	0.0462	0.0487
2.8	0.0277	0.0317	0.0343	0.0363	0.0357	0.0407	0.0442	0.0467
3.0	0.0265	0.0303	0.0330	0.0349	0.0340	0.0389	0.0423	0.0448

TABLE II: The coefficient  $C_F$  as a function of separation for the van der Waals force acting between a hydrogen atom or a molecule and single-wall carbon nanotubes of different radii.

$a$ (nm)	$C_F$ (a.u.)							
	hydrogen atom				hydrogen molecule			
	$R = 2$ nm	$R = 3$ nm	$R = 4$ nm	$R = 5$ nm	$R = 2$ nm	$R = 3$ nm	$R = 4$ nm	$R = 5$ nm
1.0	0.175	0.186	0.193	0.197	0.232	0.248	0.256	0.262
1.2	0.162	0.174	0.181	0.185	0.214	0.230	0.239	0.245
1.4	0.150	0.163	0.170	0.175	0.198	0.214	0.224	0.231
1.6	0.140	0.153	0.161	0.166	0.184	0.201	0.211	0.218
1.8	0.132	0.145	0.153	0.158	0.173	0.190	0.200	0.207
2.0	0.124	0.138	0.146	0.151	0.162	0.180	0.190	0.197
2.2	0.118	0.131	0.139	0.144	0.154	0.170	0.181	0.189
2.4	0.112	0.125	0.133	0.139	0.146	0.162	0.173	0.181
2.6	0.108	0.120	0.128	0.133	0.138	0.155	0.166	0.174
2.8	0.102	0.115	0.123	0.128	0.132	0.148	0.159	0.167
3.0	0.0975	0.110	0.119	0.124	0.126	0.142	0.153	0.161